Assembly of the Arc Repressor–Operator Complex: Cooperative Interactions between DNA-Bound Dimers†

Bronwen M. Brown and Robert T. Sauer*

Department of Biology, Massachusetts Institute of Technology, Cambridge, Massachusetts 02139

Received July 23, 1992; Revised Manuscript Received November 9, 1992

ABSTRACT: Arc repressor, a member of the β-ribbon family of DNA binding proteins, binds to its 21-base-pair operator as a tetramer. Here, the Arc dimer is shown to bind specifically to DNA fragments containing operator half-sites, and the equilibrium and kinetic constants for these reactions are determined. DNA-bound dimers are also shown to be transient intermediates in association experiments, indicating that assembly of the Arc tetramer–operator complex occurs by sequential addition of dimers to operator half-sites. When the left or right operator half-site is occupied by an Arc dimer, cooperative interactions increase the affinity of the second dimer by approximately 5900-fold [$\Delta\Delta G = -5.1$ (± 0.5) kcal/mol]. This increase in affinity is largely caused by an increase in the half-life of the complex; "non-cooperatively" bound dimers dissociate with a half-life of a few seconds while "cooperatively" bound dimers have half-lives of more than 1 h.

The three-dimensional structures of almost 20 different DNA binding proteins and/or protein–DNA complexes have now been solved, and the activities of scores of other sequence-specific DNA binding proteins have been studied by a wide range of genetic, biochemical, and biophysical methods [for reviews, see Evans (1988), Struhl (1989), Berg (1989), Harrison and Aggarwal (1990), Steitz (1990), Frankel and Kim (1991), Harrison (1991), and Pabo and Sauer (1992)]. Two themes emerge from these studies. The first is that simple structural motifs, such as the helix–turn–helix or zinc finger, often mediate direct contacts between the protein and the DNA. These motifs provide a surface that fits into the major groove of double-stranded DNA, allowing direct contacts between protein side chains and the DNA bases. The second theme is that of cooperativity. It is exceedingly rare that protein–DNA recognition is mediated by a single structural unit. Many proteins bind DNA as homodimers, heterodimers, or higher oligomers. Even when only a single protein is involved in DNA binding, there are often several independent structural domains that contact the DNA. As a result, protein–protein interactions (whether between or within molecules) almost always serve to couple the binding energies of individual DNA binding units. Understanding and characterizing the contributions of these cooperative interactions are critical to understanding fully the process of protein–DNA recognition.

We have been studying the Arc repressor of bacteriophage P22, which is a dimer at high protein concentrations but exists largely as a denatured monomer at the subnanomolar concentrations where operator DNA binding is observed in vitro (Vershon et al., 1985; Bowie & Sauer, 1989a; Brown et al., 1990). Under these conditions, operator binding is a highly cooperative, fourth-order reaction, and the Arc tetramer is the oligomeric species that is stably bound to operator DNA (Brown et al., 1990). In the solution structure of the Arc dimer, the monomers are intertwined (as opposed to being distinct globular domains) with residues 8–14 of each monomer pairing to form an antiparallel β-ribbon (Breg et al., 1990). Genetic studies indicate that the solvent-exposed residues in this β-ribbon play important roles in DNA binding (Vershon et al., 1986; Bowie & Sauer, 1989b; Knight & Sauer, 1989). The *arc* operator is a 21-base-pair sequence with an axis of approximate 2-fold rotational symmetry passing through the central base pair (Vershon et al., 1987, 1989). Thus, the operator can be thought of as being composed of symmetrically related 10-base-pair half-sites.

Model-building studies show that the β-ribbon region of an Arc dimer could fit neatly into the major groove of an operator half-site (Breg et al., 1990). The stable Arc tetramer–operator complex would thus be composed of two dimers, each bound to an operator half-site. In this model, monomer–monomer contacts are important both for formation of the β-ribbon DNA binding motif and for overall stabilization of the dimer. It also seems likely that protein–protein contacts between adjacently bound dimers are important for stabilizing the DNA-bound tetramer. Dimer–dimer contacts of this type have been directly observed in the cocrystal structure of the DNA complex of the MetJ repressor, a protein related to Arc (Somers & Phillips, 1992).

There are several possible paths for the assembly of the Arc tetramer–operator DNA complex. Two dimers could form a tetramer in solution and then bind to the DNA. Alternatively, dimers could bind sequentially to operator half-sites with tetramer formation occurring on the DNA. In this paper, we demonstrate that Arc dimers can specifically bind to operator half-sites, and determine the equilibrium constants and kinetic constants for these interactions. We show that the dimer-bound operator is a kinetic intermediate in the overall binding reaction. We also analyze thermodynamic cycles that allow estimates of the free energy of Arc tetramer formation on the DNA and argue that direct binding of solution tetramers to DNA is a kinetically insignificant reaction.

MATERIALS AND METHODS

Buffers. SB contains 50 mM Tris (pH 8.0), 0.1 mM EDTA, 5% glycerol, and 1.4 mM 2-mercaptoethanol. CB contains 50 mM Tris (pH 8.0), 100 mM KCl, 0.1 mM EDTA, and 1 mM 2-mercaptoethanol. Loading buffer for the gel mobility shift assays contains 50% glycerol in 10 mM Tris (pH 8.0),1 mM EDTA (pH 8.0). Loading buffer for DNase footprinting contains 95% formamide, 20 mM EDTA, and 0.05% xylene cyanol. Binding buffer contains 10 mM Tris (pH 7.5), 3 mM

† Supported by NIH Grant AI-16892.

0006-2960/93/0432-1354$04.00/0 © 1993 American Chemical Society

$MgCl_2$, 0.1 mM EDTA, 100 mM KCl, 100 μg/mL bovine serum albumin (BSA), and 0.02% Nonidet NP-40 (NP-40). Both BSA and NP-40 serve to reduce Arc sticking to glass and plastic surfaces at low protein concentrations. Dilution buffer is the same as binding buffer with the addition of 50% glycerol. DNase reaction buffer contains 10 mM Tris (pH 7.5), 10 mM $MgCl_2$, 1.5 mM $CaCl_2$, 0.1 mM EDTA, 50 mM KCl, 1 mM dithiothreitol, 25 μg/mL sonicated salmon sperm DNA, and 100 μg/mL BSA. DNase I storage buffer is 50% glycerol, 150 mM NaCl, 10 mM Tris (pH 7.5), and 1 mg/mL BSA. All buffer components are reagent grade. Water was distilled and deionized using a Millipore MilliQ system. PCR buffer contains 50 mM KCl and 10 mM Tris-HCl (pH 8.3) and was obtained from Perkin-Elmer Cetus in the *GeneAmp* PCR Core Reagents kit.

Protein Purification. Arc was expressed in *Escherichia coli* strain X90/pTA200 (Amman et al., 1983) and purified as described by Vershon et al. (1986) with some modifications. Cells were grown in LB broth supplemented with 150 μg/mL ampicillin. Cells were harvested and lysed, and the lysate was precipitated with poly(ethylenimine) and ammonium sulfate as described. The resuspended ammonium sulfate pellet was dialyzed in Spectra/Por 3 dialysis membrane into SB, and then chromatographed with a KCl gradient from 50 to 600 mM on a CM Accell (Waters) column using a Pharmacia FPLC. The pooled fractions were precipitated with ammonium sulfate, resuspended in CB plus 4 M GuHCl, and loaded onto a Sephadex G-75 column equilibrated in the same buffer. Fractions containing Arc were first dialyzed against 50 mM NH_4HCO_3, then dialyzed against water, and concentrated using an Amicon ultrafiltration cell. The purified sample was adjusted to 10 mM Tris (pH 7.5), 0.1 mM EDTA, and 50 mM KCl and stored in small aliquots at −20 °C. Arc-st5 was purified using essentially the same protocol and was a gift from Marcos Milla. Arc-st5 is a variant bearing five additional C-terminal amino acids with the sequence Lys-Asn-Gln-His-Glu. This tail does not affect the structure, stability, or operator affinity of Arc as assessed by biochemical experiments in vitro. Arc concentration was determined using an extinction coefficient at 280 nm of 6756 M^{-1} cm^{-1} as described (Brown et al., 1990) and is expressed as moles of Arc monomer equivalents per liter. The actual monomer or dimer concentration at a given total Arc concentration can be calculated from eq 3 and/or eq 4 (see below) and the equilibrium constant of folding and dimerization (Bowie & Sauer, 1989a).

Plasmid Construction. pAO200 and pAO250 were constructed as sources of DNA fragments for footprinting bearing, respectively, the intact operator sequence and the left half-site operator sequence. Oligonucleotides were synthesized and annealed to form the two insert cassettes (shown in Figure 1a). These cassettes and the gap linker 5′-ATTGCA-3′ were ligated into the *PstI–SmaI* backbone of pBLUESCRIPT KS(−) (Stratagene). Ampicillin-resistant transformants of *E. coli* strain X90 were selected, and the insert sequences were confirmed by dideoxy sequencing.

DNA Fragments. The operator DNA fragments used for the gel mobility shift assays and the primers used for polymerase chain reactions (PCR) were synthesized using an Applied Biosystems 381A DNA synthesizer. The oligonucleotides were purified by FPLC chromatography using an anion-exchange Mono-Q column or by gel electrophoresis following standard procedures (Maniatis et al., 1982). The sequences of DNA fragments used for binding assays are shown in Figure 1b. Fragment O1 contains the 21-base-pair wild-type *arc* operator sequence with a few flanking nucleotides. Fragments L1 and L2 contain the left half-site, and fragments R1 and R2 contain the right half-site of the operator. A 19-base-pair fragment (NS1) and a 51-base-pair fragment (NS2) were used to assay nonspecific binding. In choosing nonspecific sequences or sequences flanking operator sites, care was taken to exclude TAGA sequences as these elements seem to be critical for specific Arc binding (Vershon et al., 1989).

DNA fragments were end-labeled by kinasing one of the pair of complementary oligonucleotides using γ-^{32}P-labeled ATP and T4 polynucleotide kinase (Maniatis et al., 1982). The reaction was heat-inactivated for 10 min at 68 °C, and a 2-fold excess of the unlabeled complementary oligonucleotide was added to allow formation of the duplex DNA. The mixture was extracted once with phenol/chloroform/isoamyl alcohol (25:24:1), and the duplex was separated from the unincorporated ATP on a Sephadex G-25 spin column (Boehringer Mannheim Corp).

Fragments for use in DNase footprinting (an 80-base-pair fragment for the intact operator sequence and a 79-base-pair fragment for the left half-site sequence) were generated by PCR using kinased primers and a plasmid-derived template molecule. The two PCR primers were 5′-AGAACTAGTG-GATCC-3′ and 5′-AGCTTGATATCGAAT-3′. To obtain product radiolabeled on only one strand, in a given PCR reaction only one of the two primers was kinased. The PCR template molecules were generated by digesting pAO200 or pAO250 to completion with *ClaI* and *EagI*. The desired fragments, 88 base pairs for the intact operator and 87 base pairs for the left half-site, were then purified on a 2% agarose gel, cut out, and extracted using the Qiaex procedure (Qiagen, Inc). PCR reactions were performed using reagents from Perkin-Elmer Cetus. Each 200-μL reaction contained PCR buffer, 2.5 mM $MgCl_2$, 100 μM each of dNTP's, approximately 100 ng of template DNA, 50 pmol of each primer and 5 units of *AmpliTaq* DNA polymerase. The reactions were cycled 20 times following a cycle profile of denaturing at 94 °C for 60 s, annealing at 38 °C for 40 s, and extension at 72 °C for 60 s. The final cycle had a 10-min extension time. The autosegment extension feature of the Perkin-Elmer Cetus DNA thermal cycler was used to increase the extension time 5 s each cycle. The PCR product was purified by nondenaturing polyacrylamide gel electrophoresis, excised, eluted overnight into 250 mM NaOAc (pH 4.8), and ethanol-precipitated.

Gel Mobility Shift Assays. Gel mobility shift assays were performed essentially as described (Brown et al., 1990). Arc protein was freshly diluted in binding buffer in either polypropylene tubes or microtiter plates. Protein (0.9 of the reaction volume) was added to 0.1 volume of DNA (final concentration 8–20 pM) in microtiter plates, and reactions were incubated for a minimum of 2 h at room temperature [20 (±1) °C]. A 0.1 volume of loading buffer was added to each reaction, and 800 cpm per lane were loaded onto a nondenaturing 0.5× TBE/7% polyacrylamide gel [acrylamide: bis(acrylamide) ratio of 29:1]. No dye was used in the loading buffer added to the samples as it was found to compete for binding in the half-site operator assays. Instead, a separate lane of tracking dye (0.02% xylene cyanol and 0.02% bromophenol blue) was loaded. Gels were preelectrophoresed at 300 V for at least 30 min before being loaded. After the gels were loaded, they were electrophoresed at 300 V until the dye migrated into the gel and then at 150 V until the bromophenol blue was roughly 1 in. from the bottom of the

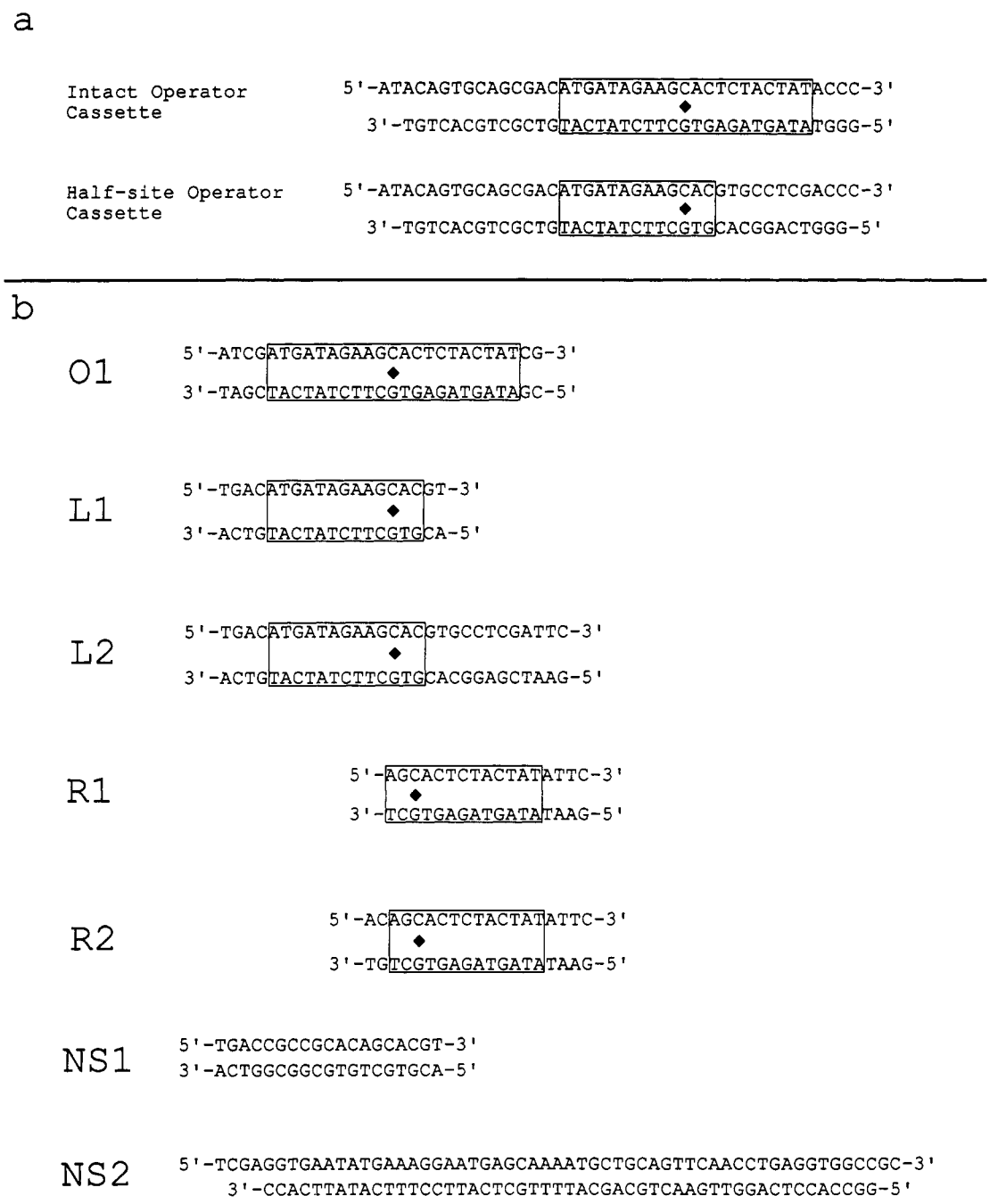

FIGURE 1: (a) Sequences of the oligonucleotide cassettes used to clone the intact *arc* operator sequence and the left half-site sequence for footprinting studies. (b) Sequences of the DNA fragments used in binding assays. Operator sequences are boxed with the central CG base pair indicated by a diamond.

gel. Gels were dried and autoradiographed, and band intensities were quantitated by densitometry (Brown et al., 1990).

For mixed oligomer assays (Brown et al., 1990), Arc and Arc-st5 were diluted to 2.2 nM in binding buffer, mixed in different ratios, heated to 68 °C for 5 min, and allowed to cool to room temperature. This protein mixture was then mixed with operator, incubated, and electrophoresed as described above. For better visualization, 1100 cpm per lane were loaded for these reactions.

In several cases, the affinity of Arc for DNA fragments was measured by competition assays. To measure the affinity of Arc for L1, labeled O1 operator (final concentration 15 pM) and different concentrations of unlabeled L1 were mixed, and then Arc protein was added to a final concentration of 0.3 nM. The reaction conditions, buffers, incubation times, and electrophoreses were as described for the gel mobility shift assay. To measure the affinity of Arc for NS2, two different experiments were performed. In the first, labeled O1 (final concentration 15 pM) and different concentrations of unlabeled NS2 were mixed, and then Arc protein was added to a final concentration of 0.28 nM. In the second experiment, labeled L1 (final concentration 15 pM) and different concentrations of NS2 were mixed, and then Arc protein was added to a final concentration of 8.0 nM. In both experiments, reactions were then incubated and electrophoresed as described for the gel mobility shift assays.

Dissociation Rates. Arc at a final concentration of 4 nM for experiments using the L1 fragment or 10 nM for experiments using the R2 fragment was incubated with 3×10^4 cpm

of DNA at room temperature. The mixture was diluted 20-fold with dilution buffer, and at different times, samples were taken and loaded onto a 0.5× TBE/7% acrylamide gel running at 300 V. After all samples were loaded, the gel was run at 150 V and processed as described above. The resulting final Arc concentration of 0.2 nM (L1) or 0.5 nM (R2) would result in less than 5% DNA bound in an equilibrium experiment.

Association Rates. Arc was diluted using binding buffer plus 5% glycerol, and the dilutions were preequilibrated in a 20 °C waterbath. Binding was initiated by adding Arc (in 0.9 of the reaction volume) to approximately 10 000 cpm of a DNA fragment (either O1, L1, or R2 in 0.1 volume) with gentle mixing, and at different times, samples were removed and loaded onto a 0.5× TBE/7% acrylamide gel running at 300 V. After all the samples were loaded, the gel was run at 150 V until the bromophenol blue was about 1 in. from the bottom of the gel. Gels were dried and band intensities quantitated either by using autoradiography and densitometry as described above or by using phosphorimagery. For the latter, the dried gel was exposed on a phosphorimager screen for 125 min. The screen was scanned on a Molecular Dynamics PhosphorImager, and the results were quantitated by volume integration using ImageQuant software. Association rate data were fit by trial and error using a computer program written to numerically integrate the linearized rate equations with a time step of 0.01 s.

DNase I Footprinting. Arc or an equivalent volume of DNase I reaction buffer was incubated with 25 000–100 000 cpm of PCR-generated DNA, in a 100-μL reaction, for at least 1 h at room temperature. A 10 μg/mL stock solution of DNase I in storage buffer was diluted to 0.2 μg/mL in DNase I reaction buffer and added to the Arc–DNA mixture at a final concentration of 9.5 ng/mL. The reaction was allowed to proceed for 18 min and was quenched by addition of 700 μL of a mixture of ice-cold ethanol and 5 M NH_4OAc (6:1 v/v). Samples were centrifuged for 30 min, and the pellet was washed with 70% ethanol and dried in a Savant Speed Vac concentrator. To obtain footprints representative of the bound complexes, samples were resuspended in binding buffer and 0.1 volume of loading buffer and electrophoresed as described for the gel mobility shift assays. The Arc–DNA complexes, containing roughly 50% of the counts, were excised, and the DNA was eluted overnight into 250 mM NaOAc (pH 4.8) at 37 °C. The eluate was ethanol-precipitated, washed with 70% ethanol, dried briefly, resuspended in 50 mL of MilliQ water, and desalted using a G-25 Sephadex spin column (Boehringer Mannheim Corp.) equilibrated in water. Samples were then dried and counted. Samples were resuspended in footprint loading buffer, heated to 90 °C for 2 min, and loaded onto an 8% denaturing acrylamide gel [acrylamide:bis-(acrylamide) ratio of 19:1] that had been preelectrophoresed for at least 1 h at 55 W. In the samples containing protein, about 8000 cpm were loaded per lane. For control DNase I reactions, 4000 cpm were loaded. Maxam and Gilbert "G"-sequencing reactions were included to allow band identification (Maxam & Gilbert, 1980).

Calculations. For the reactions shown in Figure 2

$$[A_{total}] = [U] + 2[A_2] + 4[A_4] + 2[A_{2L}O] + 2[A_{2R}O] + 4[A_4O] \quad (1)$$

where $[A_{total}]$ is the total Arc protein concentration (in monomer equivalents), [U] is the concentration of Arc monomers, $[A_2]$ is the concentration of Arc dimers, $[A_4]$ is the concentration of Arc tetramers, $[A_{2L}O]$ and $[A_{2R}O]$ are

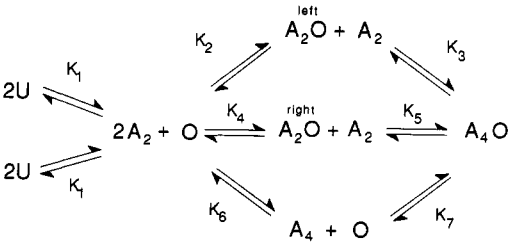

FIGURE 2: Models for Arc binding to its operator. U represents the denatured Arc monomer, O represents operator DNA, A_2 is the Arc dimer, A_2O is a dimer complex (bound either to the left half-site or to the right half-site as indicated), and A_4O is the tetramer-bound complex.

the concentrations of the Arc dimer–operator complexes where the dimer is bound to the left half-site or the right half-site, respectively, and $[A_4O]$ is the concentration of the Arc tetramer–operator complex. As discussed under Results, the concentration of free Arc tetramers is extremely low and thus can be ignored. Moreover, because Arc is always present in significant excess over total operator DNA in our experiments, the concentration of bound Arc can also be ignored. These facts allow simplification of eq 1 to

$$[A_{total}] \approx [U] + 2[A_2] \quad (2)$$

The concentration of Arc monomers and dimers is related by the equilibrium expression:

$$K_1 = [U]^2/[A_2] \quad (3)$$

Substituting $[U]^2/K_1$ for $[A_2]$ in eq 2 and solving the resulting quadratic expression give

$$[U] \approx (K_1/4)(-1 + \sqrt{1 + 8[A_{total}]/K_1}) \quad (4)$$

The binding isotherm relating the fractional saturation of a DNA site by the Arc dimer is given by

$$\theta_d = \frac{[A_2O]}{[O] + [A_2O]} = \frac{1}{1 + K_1K_2/[U]^2} \quad (5)$$

where

$$K_2 = [A_2][O]/[A_2O] \quad (6)$$

The binding isotherm relating fractional saturation of a DNA site by the Arc tetramer is given by

$$\theta_t = \frac{[A_4O]}{[O] + [A_4O]} = \frac{1}{1 + K_1^2K_{obs}/[U]^4} \quad (7)$$

where

$$K_{obs} = [A_2]^2[O]/[A_4O] \quad (8)$$

For analysis of assays in which Arc binding to competitor DNA (designated I) reduces the concentration of a small quantity of the A_4O complex, the conservation equations are

$$[A_{total}] \approx [U] + 2[A_2] + 2[A_2I] \quad (9)$$

and

$$[I_{total}] = [I] + [A_2I] \quad (10)$$

The equilibrium constant for binding of the Arc dimer to the competitor I can then be written as

$$K_i = \frac{[A_2][I]}{[A_2I]} = \left(\frac{[U]^2}{K_1}\right)\left(\frac{2[I_{total}]}{[A_{total}] + [U] - 2[U]^2/K_1} - 1\right) \quad (11)$$

where U is related to θ_t by

$$[U] = \sqrt[4]{\frac{K_1^2 K_{obs}\theta_t}{1-\theta_t}} \quad (12)$$

For analysis of assays in which Arc binding to competitor DNA reduces the concentration of a small quantity of the A_2O complex, eq 9–11 are still valid, and U is related to θ_d by

$$[U] = \sqrt{\frac{K_1 K_2 \theta_d}{1-\theta_d}} \quad (13)$$

Derivation of the competition equations assumes that the Arc dimer is the major DNA binding species and that binding of Arc to the competitor is not cooperative. In the case of nonspecific binding, two lines of evidence indicate that binding of Arc is not cooperative. First, nonspecific binding is fit extremely well by eq 11. For example, the average value of K_i calculated at five concentrations of the nonspecific competitor fragment NS2 ranging from 3.1×10^{-8} to 10^{-6} M was $2.3 (\pm 0.8) \times 10^{-8}$ M. Second, in gel shift experiments using NS2, protein–DNA complexes containing one, two, three, four, and five Arc dimers were found to have roughly equal populations at half-maximal binding (data not shown).

Error Analysis. In most cases, the values for the measured affinities and dissociation rates are the averages (±standard deviation) of three or more independent experiments. When using these values to calculate other constants, errors were propagated using the general method outlined by Bevington (1969).

RESULTS

Under equilibrium conditions, Arc binds to its operator in a reaction in which four denatured monomers combine with the operator to form a DNA-bound tetramer (Brown et al., 1990):

$$4U + O \rightleftarrows A_4O \quad (14)$$

Although this description accounts for the equilibrium properties of the reaction, it is not physically reasonable that five molecules would collide in a single kinetic step to form the protein–DNA complex. Arc dimers must play some role in the assembly process because the complex is known to form faster when Arc is added as a dimer than it does when Arc is added as a monomer (Brown et al., 1990). Figure 2 shows several plausible routes for the overall assembly of the Arc–operator complex. Each of the possible assembly paths includes the Arc dimer (A_2) and is composed of four bimolecular reactions.

We refer to the different assembly possibilities shown in Figure 2 by their unique equilibrium steps. Thus, the K_2K_3 pathway refers to the path in which one Arc dimer first binds to the left operator half-site and then a second dimer binds to the right operator half-site. The K_4K_5 pathway is similar to the K_2K_3 path except that the half-sites are filled in reverse order. In the K_6K_7 pathway, two Arc dimers combine to form a solution tetramer, which then binds to the operator.

Although the K_6K_7 path is physically reasonable, we believe that it is kinetically insignificant. Arc is dimeric at concentrations as high as 0.2 mM (Vershon et al., 1985) under conditions similar to those used in our DNA binding reactions. Hence, the equilibrium constant for tetramer formation in solution (K_6) must be greater than 0.2 mM, and there would be vanishingly small amounts of tetramer (less than 7×10^{-17} M) at the subnanomolar Arc concentrations where operator binding occurs. The initial rate at which A_4O complexes form at an Arc concentration of 10^{-9} M and an operator concentration of 5×10^{-12} M is 2.5×10^{-13} M s^{-1} (Brown et al., 1990). For preformed tetramers to account for this binding, k_7, the association rate constant for tetramer binding to the operator, would need to be greater than 4×10^{14} M^{-1} s^{-1}. However, this value is roughly 10^5-fold greater than the diffusion limit for bimolecular reactions, and thus the K_6K_7 pathway cannot be kinetically significant.

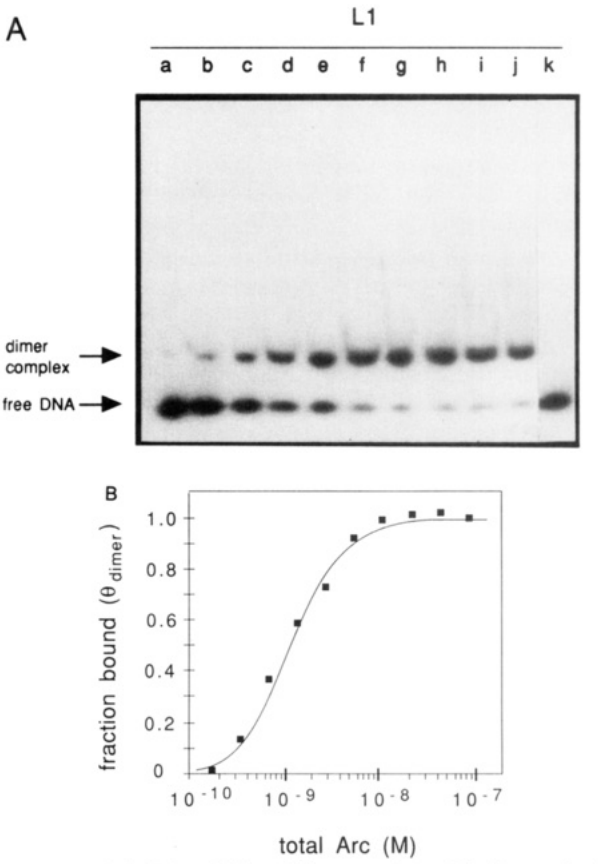

FIGURE 3: (A) Gel mobility shift assay of Arc binding to the L1 half-operator fragment. The total Arc concentration increases from left to right in 2-fold increments from lane a (1.9×10^{-10} M) to lane j (1.0×10^{-7} M). Lane k is a no-protein control. The DNA concentration in each lane is ~8 pM. (B) Binding curve of the Arc–L1 binding data from panel A. The solid line represents the equation $\theta_{dimer} = [A_2L1]/([A_2L1] + [L1]) = 1/(1 + K_1K_{2(L1)}/[U]^2)$ with $K_1 = 5 \times 10^{-9}$ M and $K_{2(L1)} = 1.6 \times 10^{-10}$ M.

Arc Binding to Half-Site Operators. To investigate the half-site binding reactions that are part of the K_2K_3 and K_4K_5 pathways, we synthesized DNA fragments containing only the left half-site or only the right half-site of the operator for use in gel mobility shift assays. The sequences of these fragments are shown in Figure 1b.

Figure 3A shows a gel mobility shift assay monitoring Arc binding to the 19-base-pair fragment containing the left operator half-site (fragment L1). There is a single bound complex with half-maximal binding at an Arc concentration of roughly 1.5 nM. A nonspecific DNA fragment of similar length (NS1) showed no complex formation over the same range of Arc concentrations (data not shown). In Figure 3B, the binding of Arc to the L1 fragment can be seen to be well fit by a theoretical curve for the second-order reaction:

$$2U + L1 \overset{K_1}{\rightleftarrows} A_2 + L1 \overset{K_{2(L1)}}{\rightleftarrows} A_2L1 \quad (15)$$

with $K_1 = 5 \times 10^{-9}$ M (Bowie & Sauer, 1989a; Brown et al.,

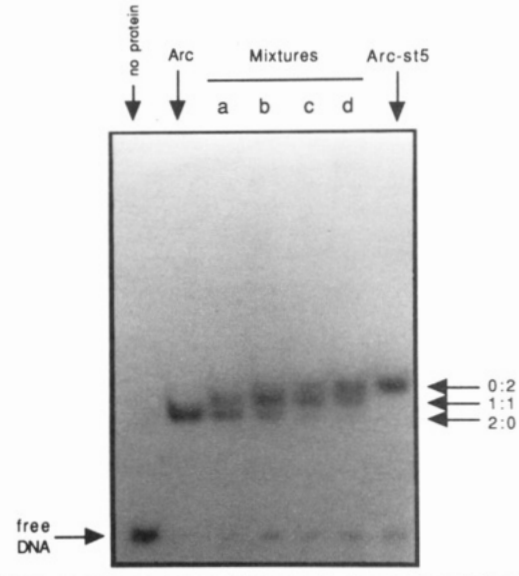

FIGURE 4: Mixed oligomer experiment. Lanes containing the L1 half-operator DNA fragment incubated with no protein, Arc, or Arc-st5 are indicated. Lanes a–d contain L1 DNA incubated with 2:1, 1:1, 1:2, and 1:3 molar ratios of Arc and Arc-st5, respectively. The total protein concentration in each assay was 2×10^{-9} M.

1990) and $K_{2(L1)} = 1.6 \times 10^{-10}$ M. In repeats of this binding experiment, values for $K_{2(L1)}$ of 3.2×10^{-10} and 4.5×10^{-10} M were obtained. We take the average of these values [3.1 ($\pm$1.5) $\times 10^{-10}$ M] as the equilibrium constant for dissociation of the Arc dimer from the left operator half-site. As an independent method of measuring Arc binding to L1, the affinity was also determined by using the L1 fragment to compete for Arc binding to the intact operator (O1). This method yielded a $K_{2(L1)} = 3.5 \times 10^{-10}$ M, which is within error of the average value calculated from the gel mobility shift experiments.

To confirm that Arc binds to the L1 fragment as a dimer, the gel mobility shift assay was repeated using a mixture of Arc and Arc-st5, a longer but fully active variant. As seen in Figure 4, three different protein–DNA complexes are detected. The fastest and slowest migrating complexes comigrate with the bound complexes of Arc and Arc-st5, respectively. The presence of a single intermediate is consistent with a dimer being the species that binds to the operator half-site (Hope & Struhl, 1987).

Two operator fragments, R1 and R2, containing the right half-site were synthesized, and binding was tested. These two operators are 17-base-pair and 19-base-pair fragments, respectively. As with the left half-site, the binding of Arc to the right half-site is a second-order reaction. The binding constant of the Arc dimer for R1 [$K_{2(R1)}$] was 1.5 ($\pm$0.9) $\times$ 10^{-9} M (average of three experiments) while for R2 $K_{2(R2)}$ was 8.8 ($\pm$1.0) $\times$ 10^{-10} M (average of four experiments).

A second fragment (L2) bearing the left half-site with adjacent nonspecific sequences was also synthesized. This fragment contains 29 base pairs, making it comparable in length to the intact operator, fragment O1. Arc binding to the L2 and O1 operator fragments is shown in Figure 5. Binding to the intact operator, O1, results in a single bound species previously shown to be a tetramer (Brown et al., 1990). Binding to L2 results in two bound complexes. The slower migrating complex comigrates with the Arc tetramer–O1 complex. A mixed-oligomer assay confirmed that the faster migrating complex is a dimer (not shown). The dissociation constant for binding of the first Arc dimer to L2 [$K_{2(L2)}$] is 5.3 ($\pm$3.9) $\times$ 10^{-10} M (average of four experiments). The

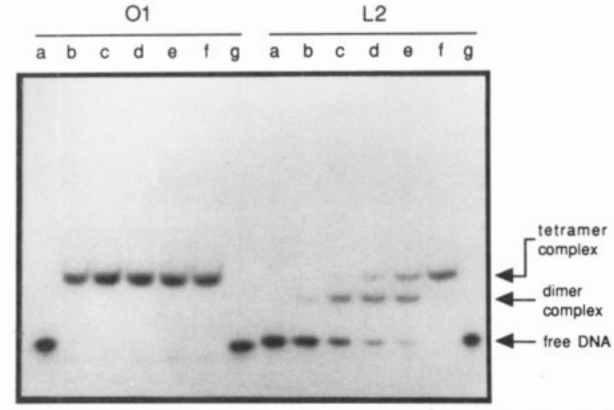

FIGURE 5: Gel mobility shift assays of Arc binding to the O1 operator fragment (left side) or L2 half-operator fragment (right side). The total Arc protein concentration in lanes a–f is 8.0×10^{-11}, 8.0×10^{-10}, 1.6×10^{-9}, 3.2×10^{-9}, 6.4×10^{-9}, and 2.6×10^{-8} M, respectively. Lane g is a no-protein control. The DNA concentration in each lane is $\sim$11 pM.

Table I: Summary of Affinities and Rate Constants[a]

operator	length (bp)	dimer affinity
L1	19	3.1 ($\pm$1.5) $\times$ 10^{-10} M
L2	29	5.3 ($\pm$3.9) $\times$ 10^{-10} M
R1	17	1.5 ($\pm$0.9) $\times$ 10^{-9} M
R2	19	8.8 ($\pm$1.0) $\times$ 10^{-10} M

equilibrium	rate	value
K_2		3.1×10^{-10} M
	k_2	1.1×10^{9} M^{-1} s^{-1}
	k_{-2}	0.35 s^{-1}
K_3		1.5×10^{-13} M
	k_3	5.5×10^{8} M^{-1} s^{-1}
	k_{-3}	8.2×10^{-5} s^{-1}
K_4		8.8×10^{-10} M
	k_4	3.0×10^{8} M^{-1} s^{-1}
	k_{-4}	0.26 s^{-1}
K_5		5.2×10^{-14} M
	k_5	1.5×10^{9} M^{-1} s^{-1}
	k_{-5}	8.2×10^{-5} s^{-1}

[a] The top section shows the affinities of the Arc dimer for the different half-sites used in gel mobility shift assays. The bottom section is a summary of the average values determined or calculated for the equilibrium and rate constants of the K_2K_3 and K_4K_5 pathways shown in Figures 2 and 9. The value used for K_1 was 5×10^{-9} M (Bowie & Sauer, 1989a; Brown et al., 1990).

binding constant for the second dimer binding to the dimer–L2 complex is 1.8 ($\pm$0.6) $\times$ 10^{-9} M (average of four experiments). We assume the first dimer is bound specifically and the second dimer binds nonspecifically to the adjacent DNA sequences. This interpretation is supported by the finding that the slower migrating complex is not observed in the presence of sonicated salmon sperm DNA at a concentration of 4.3 μg/mL (data not shown).

Table I, top section, is a summary of the binding data for the different half-site fragments. There is less than a 2-fold difference in affinities between the two different length operators for each half-site (L1 and L2, and R1 and R2). This observation indicates that the measured affinities have no significant dependence on the length of the operators used. The affinity for the right half-site appears to be slightly less than that for the left half-site. This minor difference in relative affinities presumably reflects the fact that the left and right half-sites are not identical in sequence.

Footprinting. Figure 6A shows the DNase I footprint of Arc on DNA fragments bearing the intact operator sequence or the left half-site sequence. Under the conditions of the

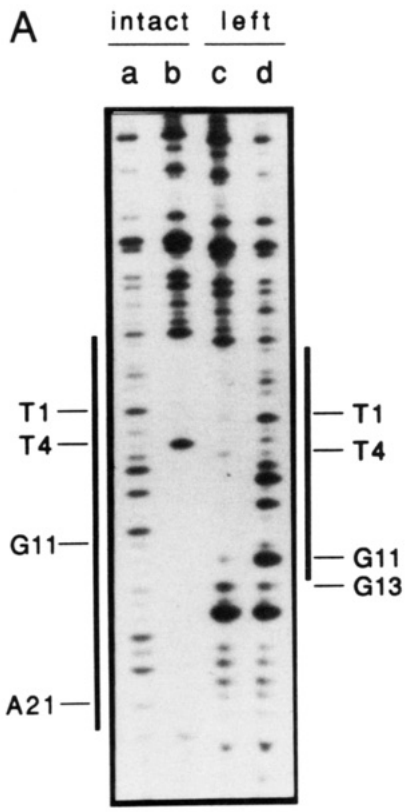

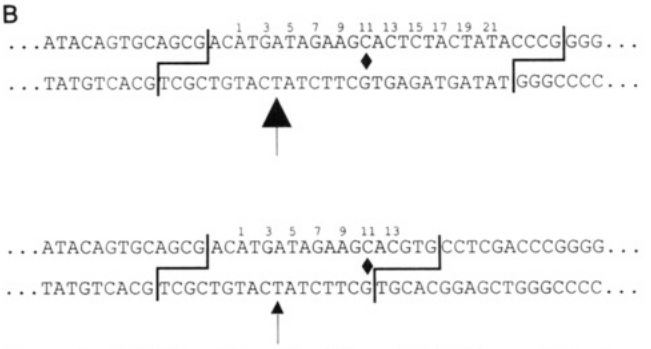

FIGURE 6: (A) DNase I footprint of Arc on DNA fragments bearing the intact operator sequence or left half-operator sequence. Lanes a and d are no-protein controls. Lanes b and c show the pattern of cleavage in the presence of 8×10^{-7} M total Arc protein. The DNA fragments (3 nM) were labeled at the 5′ end and correspond to the bottom strands shown in Figure 1a. Footprinting reactions were performed in the presence of 25 μg/mL sonicated salmon sperm DNA. (B) Summary of the DNase protection data. The extent of protection from cleavage on each sequence is indicated by the bracketed area. Operator bases are numbered. The position of Arc-mediated enhancement of DNase I cleavage in the intact operator is marked by an arrow.

footprinting assay (25 μg/mL sonicated salmon sperm DNA), control gel mobility shift experiments showed only a dimer complex with the half-site fragment. The footprint of the tetramer on the intact operator is seen in lane b and that of the dimer on the half-site in lane c. As expected, the dimer footprint is less extensive than the tetramer footprint. Note also that the enhancement in DNase cleavage seen at T4 for the tetramer-bound operator is greatly reduced in the dimer-bound complex. In the experiment shown, the bottom DNA strand was labeled. Footprinting with the upper strand labeled was also performed (data not shown). Figure 6B shows schematically the extent of protection on both strands. The tetramer footprint is roughly centered over the 2-fold axis of the operator (base 11). The dimer footprint is roughly centered at base 5 or between bases 5 and 6 of the left half-site.

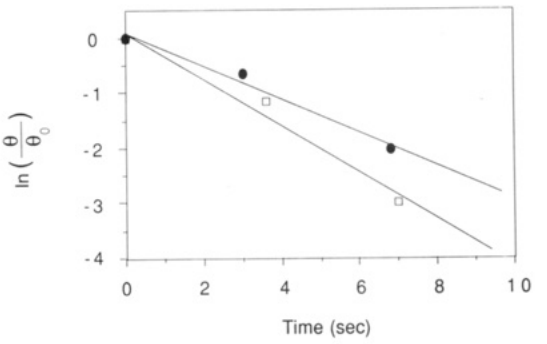

FIGURE 7: Dissociation of DNA complexes between Arc dimers and the L1 (□) and R2 (●) half-operator fragments. Time is counted from the loading of the first dissociation time point on the gel (protein and DNA were mixed ~3 s before). The solid lines represent the equation $\ln(\theta/\theta_0) = -k_{off}t$ with $k_{off} = 0.42\ s^{-1}$ for L1 and $k_{off} = 0.30\ s^{-1}$ for R2.

Dissociation Kinetics. The rates of dissociation of the Arc dimer from the L1 and R2 half-site fragments were measured following rapid dilution of protein–DNA complexes (see Figure 7). For L1, the dissociation rate constant is $\sim 0.35\ s^{-1}$ (estimated error ± 0.10), corresponding to a half-life of 2 s. For R2, the dissociation rate constant is $\sim 0.26\ s^{-1}$ (estimated error ± 0.05), corresponding to a half-life of 2.7 s. The half-life of the tetramer bound to the intact operator is ~70 min, measured under similar conditions (Vershon et al., 1987; Brown et al., 1990). Thus, the bound tetramer is considerably more long-lived than the bound dimer.

Association Kinetics. The rate of association of Arc with the L1 half-operator fragment was measured by mixing the protein (at concentrations from 0.5 to 1.4 nM) and DNA and then loading portions of the mixture onto a running gel at different times. Values for the association rate constants were then determined by numerical fitting of the resulting concentration versus time data (see Materials and Methods). For these calculations, dissociation of the half-operator complexes is a significant reaction, even at early times, and was included in the numerical fitting protocol using the dissociation rate constants measured above. An example of an association experiment is shown in Figure 8A. The experimentally determined association rate constant for the Arc dimer binding to L1 was 9.8 (±6.9) × $10^8\ M^{-1}\ s^{-1}$. An independent value of 1.1 (±0.6) × $10^9\ M^{-1}\ s^{-1}$ was calculated for this association rate constant by dividing the dissociation rate constant by the equilibrium dissociation constant. The association rate constant for the Arc dimer binding to the R2 fragment was calculated to be 3.0 (±0.7) × $10^8\ M^{-1}\ s^{-1}$. These second-order rate constants are all close to the diffusion limit.

Association rate experiments were also performed using Arc and the intact operator fragment O1. As shown in Figure 8B, dimer-bound intermediates are detected at early time points and are chased into the tetramer-bound complex as a function of time. The transient presence of dimer-bound intermediates in the assembly of the tetrameric complex provides strong support for the model in which assembly occurs by sequential addition of dimers to the operator. Furthermore, the kinetic values used to calculate the theoretical curves in Figure 8B (see figure legend) are close to those measured in other half-site or whole-site experiments (see lower section, Table I). This observation indicates that the dimer-bound operator is a kinetically significant intermediate in the assembly of the Arc tetramer–O1 complex.

Analysis of Cooperative Binding Energy. A model illustrating the sequential binding of two Arc dimers to intact operator is shown in Figure 9. We assume that K_2 is equal

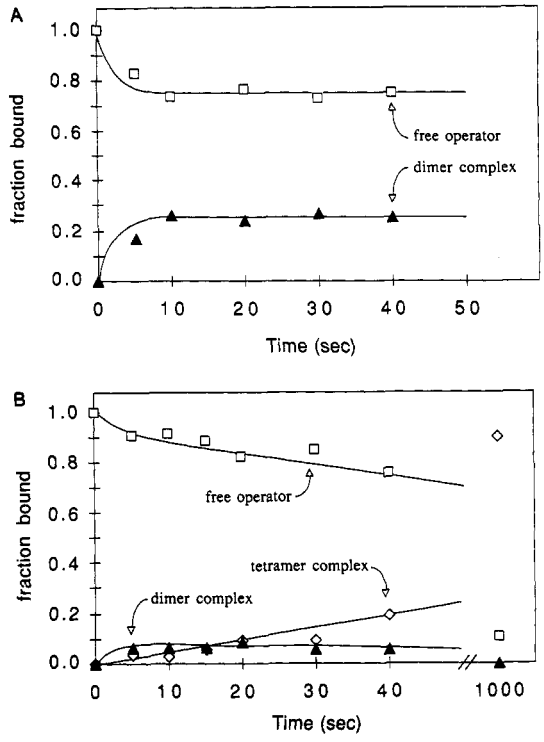

FIGURE 8: Association kinetics for Arc–DNA binding. (A) Arc binding to half-site fragment L1. Data for free operator and dimer bound-operator are as indicated. The curves are those expected using the rate constants $k_2 = 6 \times 10^8$ M^{-1} s^{-1} and $k_{-2} = 0.35$ s^{-1}. The total Arc concentration was 1.4×10^{-9} M. The total operator concentration was ~10 pM. (B) Arc binding to intact operator fragment O1. Data for free operator, dimer-bound operator, and tetramer bound-operator are as indicated. The curves are those expected using the K_2K_3 and K_4K_5 pathways of Figure 2 with the rate constants $k_2 = 6 \times 10^8$ M^{-1} s^{-1}, $k_{-2} = 0.3$ s^{-1}, $k_3 = 1.5 \times 10^9$ M^{-1} s^{-1}, $k_{-3} = 8 \times 10^{-5}$ s^{-1}, $k_4 = 3 \times 10^8$ M^{-1} s^{-1}, $k_{-4} = 0.3$ s^{-1}, $k_5 = 3 \times 10^9$ M^{-1} s^{-1}, and $k_{-5} = 8 \times 10^{-5}$ s^{-1}. The total Arc concentration was 5.0×10^{-10} M. The total operator concentration was ~10 pM.

to $K_{2(L1)}$ and that K_4 is equal to $K_{2(R2)}$. A value of $K_{obs} = 4.5$ ($\pm$2.7) $\times 10^{-23}$ M^2 [average of five experiments; data not shown, but see Brown et al. (1990) for comparable data] was measured by analysis of Arc binding to the O1 fragment. Because the top and bottom portions of the figure represent thermodynamic cycles, values for $K_3 = K_{obs}/K_2 = 1.5$ ($\pm$1.1) $\times 10^{-13}$ M and $K_5 = K_{obs}/K_4 = 5.2$ ($\pm$3.1) $\times 10^{-14}$ M can be calculated. Note that K_2 represents binding of the Arc dimer to the left half-site when the right half-site is free while K_5 represents binding of a dimer to the left site when the right half-site is occupied. A similar relationship for binding to the right half-site holds true for K_4 and K_3. Thus, the ratio $K_2/K_5 = K_4/K_3 = 5.9$ ($\pm$4.7) $\times 10^3$ represents the cooperative enhancement in binding of the second dimer when the left or right half-site is already occupied.

Nonspecific Binding. The affinity of Arc for nonspecific DNA was measured using two fragments, NS1 and NS2. The binding of Arc to NS1 [$K_{2(NS1)} = 1.8 \times 10^{-7}$ M] was measured by monitoring the loss of free DNA using a gel mobility shift assay (no discrete bound band was detected with the NS1 fragment). The binding of Arc to NS2 was measured by a competition assay against the A_4O complex [$K_{2(NS2)} = 2.3 \times 10^{-8}$ M] or the A_2L1 complex [$K_{2(NS2)} = 3.5 \times 10^{-8}$ M]. The $K_{2(NS1)}$ and $K_{2(NS2)}$ affinity values cited are macroscopic equilibrium constants. The corresponding microscopic equilibrium constants (K_{site}) can be calculated by assuming that NS1 has 9 identical nonspecific sites of 10 base pairs and NS2 has 40 such nonspecific sites. The K_{site} values from the three experiments are 1.6×10^{-6}, 9.2×10^{-7}, and 1.4×10^{-6} M,

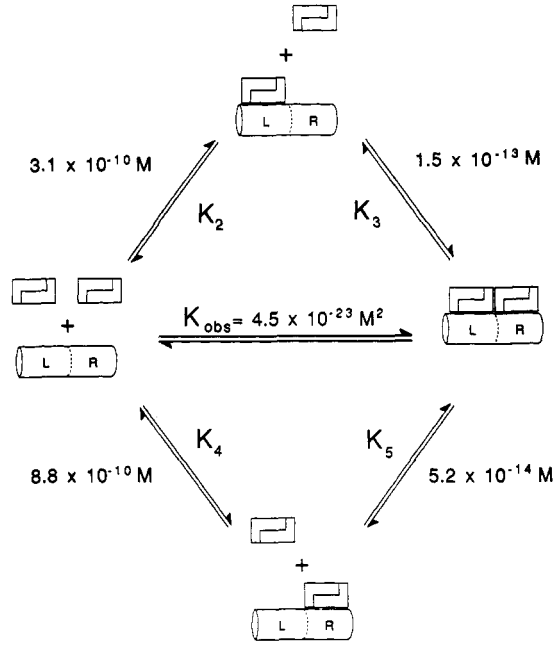

FIGURE 9: Thermodynamic cycles for analysis of cooperative binding of Arc dimers to operator DNA. K_2 and K_4 are assumed to be equal to $K_{2(L1)}$ and $K_{2(R2)}$, respectively. K_{obs} is the average second-order equilibrium constant for binding of two Arc dimers to the intact operator. $K_3 = K_{obs}/K_2$. $K_5 = K_{obs}/K_4$. The affinity of Arc for the left or right half-site is increased by approximately 5900-fold when the other half-operator site is occupied.

respectively. We take the average of these values [1.3 ($\pm$0.4) $\times 10^{-6}$ M] as a reasonable estimate of the affinity of the Arc dimer for a single nonoperator site.

DISCUSSION

Oligomerization is an extremely common theme in protein–DNA interactions. The Arc repressor of phage P22 exists as an equilibrium mixture of denatured monomers and native dimers in solution (Bowie & Sauer, 1989) and as a tetramer when bound to its 21-base-pair operator (Brown et al., 1990). Although monomers are the predominant species at the low concentrations where operator binding is observed, there is no evidence that they bind to operator DNA. The dimer is the kinetically significant species in terms of DNA binding (Brown et al., 1990), presumably because the β-ribbon DNA binding motif of Arc is only formed in the dimer (Breg et al., 1990). Here, we have shown that Arc dimers bind specifically to DNA fragments containing half-operator sites. Moreover, dimer complexes with the intact operator appear as transient kinetic intermediates in association experiments. These observations suggest that assembly of the tetramer–operator complex occurs by the sequential addition of two dimers as shown in the K_2K_3 and K_4K_5 pathways of Figure 2. Microscopic reversibility dictates that the disassembly of the bound tetramer will occur by the reverse of the assembly process, i.e., by sequential dissociation of the two dimers. We have not ruled out the K_6K_7 path, in which solution tetramers bind directly to the operator or dissociate directly from the operator, but have argued that the flux through these pathways must be kinetically insignificant.

Comparisons of the half-operator and whole-operator binding affinities of Arc indicate that when a half-site is occupied by an Arc dimer, cooperative interactions enhance the binding affinity of the second Arc dimer between 1200-fold and 10 600-fold. This can be seen by comparing the K_2 and K_5, or K_4 and K_3, terms in Figure 9. Because of this

cooperative stabilization, dimer complexes are thermodynamically unstable relative to tetramer complexes, and in binding assays using the intact operator, only the tetramer complex is observed at equilibrium. The complexes between Arc dimers and half-operator fragments were found to be short-lived, with half-lives of a few seconds. In contrast, the complex between the Arc tetramer and the intact operator is considerably more long-lived, with a half-life of 70 min. The dissociation of the "cooperatively" bound dimer (i.e., the k_{-3} and k_{-5} steps in Figure 2) will be rate-limiting for dissociation of the tetramer complex. If we assume that $k_{-3} = k_{-5}$ (this is reasonable since $k_{-2} \approx k_{-4}$), then each of these dissociation rate constants would have a value of 8.2×10^{-5} s^{-1}. Comparison of these values with those estimated for the k_{-2} and k_{-4} steps from the half-operator data indicates that a "cooperatively" bound dimer is roughly 4000-fold more long-lived than a "non-cooperatively" bound dimer. Thus, kinetic stabilization largely accounts for the enhancement in the binding affinity of the second dimer in the tetramer–operator complex.

The difference in the dissociation rates of the tetramer and the dimer complexes may also be germane to the observed effect of dyes in the equilibrium binding assays. The presence of the bromophenol blue and xylene cyanol dyes in the loading buffer for the gel shift assays was found to greatly reduce the apparent affinity of Arc for the half-site fragments. This effect, however, was not observed in assays of Arc binding to the intact operator. We assume that the dyes compete by binding to either the free protein or free DNA. In the few minutes between addition of the loading buffer to the Arc–operator complexes and loading the samples onto a gel, most of the dimer-bound complexes would dissociate and reassociate repeatedly and thus be susceptible to competition whereas almost none of the tetramer-bound complexes would dissociate and thus be at risk.

The free energy change ($\Delta\Delta G$) of dimer–dimer cooperativity can be calculated as $-RT \ln (K_2/K_5)$ or -5.1 (± 0.5) kcal/mol. This value can be viewed as representing the free energy change associated with formation of the DNA-bound Arc tetramer from two DNA-bound Arc dimers. A common mistake is to attempt to equate this unimolecular free energy with that expected for formation of an Arc tetramer from two dimers in solution, but this ignores the translational and rotational entropy costs, which can be as high as 10–15 kcal/mol (Jencks, 1981), required to position two Arc dimers in solution. On the DNA, these entropic costs are largely paid by the energy of dimer binding to the operator half-sites.

In assays using the L2 half-operator fragment, we observed a complex that appears to consist of a specifically bound dimer and a nonspecifically bound dimer. In this case, the affinity of the nonspecifically bound dimer was about 2×10^{-9} M, but for DNA fragments such as NS1 and NS2, the microscopic equilibrium constant (K_{site}) is approximately 1.3×10^{-6} M. Hence, there would also appear to be cooperative enhancement in the affinity of the nonspecifically bound dimer in the L2 tetramer complex. A somewhat analogous situation has been observed in the cocrystal of an 86 amino acid fragment of the glucocorticoid receptor bound to a DNA recognition site (Luisi et al., 1991). In this case, the bound dimer consists of one specifically bound monomer and one nonspecifically bound monomer, with extensive protein–protein contacts apparently stabilizing the complex. We note, however, that there is no apparent dimer–dimer cooperativity when Arc binds to nonspecific DNA. As a result, cooperative interactions are likely to require at least some specific protein–DNA interactions.

The structure of the complex of the Arc tetramer and operator DNA is not currently known. However, MetJ repressor, a homolog of Arc, also binds to operator DNA as a tetramer (Somers & Phillips, 1992). In this case, the cocrystal structure shows helix–helix packing interactions between the MetJ dimers bound to the two operator half-sites and also reveals that the operator DNA is bent around the protein. Thus, MetJ cooperativity may well result from a combination of protein–protein contacts and from conformational changes in the DNA (Somers & Phillips, 1992). The *met* and *arc* operators are different in terms of size and half-site spacing, and thus there is no reason to assume that Arc will use the same mechanism of cooperativity as MetJ. Nevertheless, it is interesting that enhanced cleavage is observed between bases 3 and 4 in the DNase I footprint of the Arc tetramer–operator complex (see Figure 6A; Vershon et al., 1987). Since DNase I is sensitive to the width of the minor groove (Drew, 1984; Drew & Travers, 1984), this may suggest that the Arc tetramer also bends or kinks the operator DNA, thereby altering the width of the minor groove. It is important to note, however, that the enhanced DNase I cleavage is markedly reduced in the Arc dimer–operator complex and thus the putative bending would seem to be a consequence of the binding of the second dimer binding rather than a prelude to it.

If protein–protein contacts are involved in stabilizing the bound Arc tetramer, then there should be a class of Arc mutants that are defective in cooperativity. A pure cooperativity mutant should bind with wild-type affinity and kinetics to half-site operators, but with an increased dissociation rate and reduced affinity to the intact operator. We are presently screening a collection of Arc mutants that are defective in operator binding in vivo (Vershon et al., 1986) for variants with this phenotype.

In the intact *arc* operator, there is an axis of approximate 2-fold symmetry through the central CG base pair of the 21-base-pair site that is evident both in the DNA sequence and in the patterns of chemical and enzymatic protection afforded by bound Arc (Vershon et al., 1987, 1989; Knight & Sauer, 1989). There is also a second set of symmetry axes evident in the footprint data which pass between bases 5 and 6, and 15 and 16. The roughly symmetrical contacts within each half-site are consistent with our model in which a symmetric Arc dimer binds to each half-site. The DNA sequence of each half-site, however, shows little obvious symmetry. It may be that Arc cannot make fully symmetric contacts within a DNA half-site for reasons of tertiary or quaternary structure and that it actually binds with maximal affinity to asymmetric half-site sequences such as those found in the wild-type operator. Alternatively, the wild-type operator sequence may not have been selected for maximal affinity. It should be possible to address these issues using methods to select high-affinity binding sites in vitro (Blackwell & Weintraub, 1990).

ACKNOWLEDGMENT

We thank Miriam Garland and Carl O. Pabo for personal communications that suggested that Arc dimers might bind to operator half-sites. We thank John Reidhaar-Olson for advice concerning error analysis and Marcos Milla for the gift of the purified Arc-st5 protein.

REFERENCES

Amman, E., Brosius, J., & Ptashne, M. (1983) *Gene 25*, 167–178.

Berg, J. M. (1990) *Annu. Rev. Biophys. Biophys. Chem. 19*, 405–421.

Bevington, P. R. (1969) *Data Reduction and Error Analysis for the Physical Sciences*, McGraw-Hill, New York.

Blackwell, T. K., Kretzner, L., Blackwood, E. M., Eisenman, R. N., & Weintraub, H. (1990) *Science 250*, 1149–1151.

Bowie, J. U., & Sauer, R. T. (1989a) *Biochemistry 28*, 7139–7143.

Bowie, J. U., & Sauer, R. T. (1989b) *Proc. Natl. Acad. Sci. U.S.A. 86*, 2152–2156.

Breg, J. N., Boelens, R., George, A. V. E., & Kaptein, R. (1989) *Biochemistry 28*, 9826–9833.

Breg, J. N., van Opheusden, J. H. J., Burgering, M. J. M., Boelens, R., & Kaptein, R. (1990) *Nature 346*, 586–589.

Brown, B. M., Bowie, J. U., & Sauer, R. T. (1990) *Biochemistry 29*, 11189–11195.

Drew, H. R. (1984) *J. Mol. Biol. 176*, 535–557.

Drew, H. R., & Travers, A. A. (1984) *Cell 37*, 491–502.

Evans, R. M. (1988) *Science 240*, 889–895.

Frankel, A. D., & Kim, P. S. (1991) *Cell 65*, 717–719.

Harrison, S. C. (1991) *Nature 353*, 715–719.

Harrison, S. C., & Aggarwal, A. K. (1990) *Annu. Rev. Biochem. 59*, 933–969.

Hope, I. A., & Struhl, K. (1987) *EMBO J.6*, 2781–2784.

Jencks, W. P. (1981) *Proc. Natl. Acad. Sci. U.S.A. 78*, 4046–4050.

Knight, K. L., & Sauer, R. T. (1989) *Proc. Natl. Acad. Sci. U.S.A. 86*, 797–801.

Luisi, B. F., Xu, W. X., Otwinowski, Z., Freedman, L. P., Yamamoto, K. R., & Sigler, P. B. (1991) *Nature 352*, 497–479.

Maniatis, T., Fritsch, E. F., & Sambrook, J. (1982) *Molecular Cloning: A Laboratory Manual*, Cold Spring Harbor Laboratory Press, Cold Spring Harbor, NY.

Maxam, A. M., & Gilbert, W. (1980) *Methods Enzymol. 65*, 499–559.

Pabo, C. O., & Sauer, R. T. (1992) *Annu. Rev. Biochem. 61*, 1053–1095.

Phillips, S. E. V., Manfield, I., Parsons, I., Davidson, B. E., Rafferty, J. B., Somers, W. S., Margarita, D., Cohen, G. N., Saint-Girons, I., & Stockley, P. G. (1990) *Nature 341*, 711–715.

Rafferty, J. B., Somers, W. S., Saint-Girons, I., & Phillips, S. E. V. (1990) *Nature 341*, 705–710.

Scott, M. P., Tamkun, J. W., & Hartzell, G. W. (1989) *Biochim. Biophys. Acta 989*, 25–48.

Somers, W. S., & Phillips, S. E. V. (1992) *Nature 359*, 387–393.

Steitz, T. A. (1990) *Q. Rev. Biophys. 23*, 205–280.

Struhl, K. (1989) *Trends Biol. Sci. 14*, 137–140.

Vershon, A. K., Youderian, P., Susskind, M. M., & Sauer, R. T. (1985) *J. Biol. Chem. 260*, 12124–12129.

Vershon, A. K., Bowie, J. U., Karplus, T. M., & Sauer, R. T. (1986) *Proteins: Struct., Funct., Genet. 1*, 302–311.

Vershon, A. K., Liao, S., McClure, W. R., & Sauer, R. T. (1987) *J. Mol. Biol. 195*, 323–331.

Vershon, A. K., Kelley, R. D., & Sauer, R. T. (1989) *J. Biol. Chem. 264*, 3267–3273.